

Alignment-Induced Epitaxial Transition in Organic-Organic Heteroepitaxy

Dong Guo,* Kenji Sakamoto, and Kazushi Miki

Organic Nanomaterials Centre, National Institute for Materials Science, 1-1 Namiki, Tsukuba, Ibaraki 305-0044, Japan

Susumu Ikeda and Koichiro Saiki

Department of Complexity Science and Engineering, The University of Tokyo, Kashiwanoha 5-1-5, Kashiwa, Chiba 277-8561, Japan

(Received 28 July 2008; published 4 December 2008)

We report the epitaxial growth of thin films of a small organic molecule (pentacene) on polymer substrates with controllable photoalignment over a wide range. The pentacene molecular plane exhibited a distinct orientational change from *parallel* to *perpendicular* relative to the polymer chain with increasing substrate polymer alignment. Each orientation consists of twinlike domains. Such characteristics reveal a unique alignment-induced epitaxial transition controlled by the subtle balance of weak interactions, showing a promising approach for tuning the characteristics of organic semiconductor based electronic devices.

DOI: 10.1103/PhysRevLett.101.236103

PACS numbers: 68.55.am, 68.37.Yz, 81.05.Hd, 81.15.Hi

As a promising complement to mainstream inorganic semiconductors for applications requiring large area, low-temperature processing and low cost, organic semiconductors have attracted intense scientific and technological interest [1–3]. The realization that the performance of the relevant devices is inherently associated with the microstructure of the organic heterojunctions has stimulated numerous studies in organic semiconductor growth [4]. Because of the large size, anisotropy, and relatively weak van der Waals interaction of organic molecules, their growth is far more complex than that of inorganic materials, and the physical principles are still far from being well established. Studies on organic-inorganic heteroepitaxy (OIHE) have revealed that commensurism is not a prerequisite [5] and the equilibrium structure is dependent on a delicate balance of various noncovalent weak interactions [6]. Comparatively, the scenario of the rarely studied organic-organic heteroepitaxy (OOHE) is much less understood. OOHE may exhibit new epitaxy modes and its investigation may reveal interesting growth physics [7–9]. A challenging case is organic semiconductor on polymer, which is promising for “all-organic” devices such as flexible displays and sensors. Owing to the many possible configurations and conformations and the partial crystallinity of the polymer, the interactions at the interface are more complicated and it is difficult to assess and distinguish the role of different factors, such as topological effects, intermolecular interactions and lattice matching, in controlling the admolecule orientation. To clarify the ordering mechanisms in such an OOHE system, a quantitative relationship between the admolecule orientation and the polymer alignment degree is particularly useful. The objective is to prepare polymer substrates with a wide range of controllable alignment, while excluding the influence of the morphological and chemical change of the polymer surface.

In this Letter, we investigate the molecular beam epitaxy growth of pentacene, a model small molecule organic semiconductor [4] using photoaligned films of azobenzene-containing polyimide [Azo-PI, see Fig. 1(a)] as substrates. A unique feature of these substrate films is that the polymer alignment can be controlled over a wide range while changes in the surface chemical and morphological nature are substantially avoided [10]. We demonstrate a unique alignment-induced epitaxial transition, that is from control by van der Waals interactions on relatively weakly aligned polymer substrates to control by coincident epitaxy on highly aligned polymer substrates. The finding

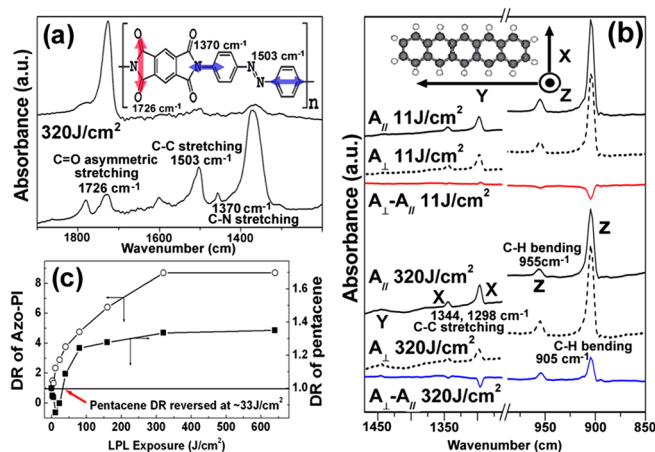


FIG. 1 (color online). (a) Polarized IR spectra of the Azo-PI film with a LPL exposure of 320 J/cm². The inset shows the molecular structure of Azo-PI and the assignment of the bands. (b) Polarized IR spectra of the pentacene films on 11 J/cm² and 320 J/cm² exposed Azo-PI. The inset shows the definition of 3 molecular axes. (c) LPL exposure dependence of DR (A_{\perp}/A_{\parallel}) of the Azo-PI films (1370 cm⁻¹ band) and the pentacene films (905 cm⁻¹ band).

demonstrates a promising approach for tuning the performance of the relevant devices, such as to control anisotropic charge transport in organic thin film transistors and polarized light emission from organic light emitting diodes.

The films of a polyamic acid containing azobenzene in the backbone (Azo-PAA) were spin-coated onto *n*-type Si wafers with a 300 nm SiO₂ layer, and then irradiated with linearly polarized light (LPL) of wavelength 340 ~ 500 nm at normal incidence [9]. The LPL exposure was varied up to 640 J/cm² to induce different degree of alignment. Here we focus on two films irradiated with 11 and 320 J/cm². Then the photoaligned Azo-PAA films were thermally converted into chemically and optically stable Azo-PI films (11 nm thick). All the pentacene films (30 nm) were deposited at a rate of 0.3 nm/min in a vacuum of ~10⁻⁵ Pa. Polarized infrared (IR) spectra were measured to assess the average orientation degree. Grazing incidence x-ray diffraction (GIXD) and specific x-ray irradiation area calibrated azimuthal scans were used to determine the detailed in-plane structure by using a Rigaku Ultima III diffractometer with a 5-axis goniometer, with which out-of-plane XRD patterns were also obtained.

The polarized IR spectra of a bare photoaligned Azo-PI film (320 J/cm²) are shown in Fig. 1(a) [11], where $A_{//}$ and A_{\perp} represent the absorbance for the IR light polarized parallel and perpendicular to the LPL polarization direction, respectively. Since the 1370 and 1503 cm⁻¹ bands are polarized along the Azo-PI chain [11], their polarization dependence of $A_{\perp} > A_{//}$ indicates that the Azo-PI is on average aligned perpendicular to the LPL polarization direction. Figure 1(b) shows the polarized IR of two typical pentacene films on photoaligned Azo-PI films, the molecular axis definition (*XYZ*) and the band assignment [12,13]. The polarization dependence of $A_{\perp} < A_{//}$ for the Z-axis bands and $A_{\perp} > A_{//}$ for the X-axis bands of the 11 J/cm² sample indicates that the molecular plane normal is oriented parallel to the LPL polarization direction, i.e., perpendicular to the Azo-PI. Surprisingly, the opposite polarization dependence of the same bands of the 320 J/cm² sample reveals a 90° orientation change with the molecular plane here oriented perpendicular to the Azo-PI. The ratio of the total absorbance ($A_{//} + A_{\perp}$) of the Y-axis band to that of the Z-axis band for both samples (0.015) is much smaller than that (0.08–0.09) of randomly orientated pentacene [13,14], indicating that the Y-axis is oriented nearly perpendicular to the surface. The dichroic ratio (DR = $A_{\perp}/A_{//}$) of Azo-PI first monotonically increases with the exposure [Fig. 1(c)], then it gradually saturates, implying a constant polymer alignment direction. In sharp contrast, the pentacene DR shows a remarkable reversal with a minimum at 11 J/cm² before saturation, revealing that the pentacene molecular plane undergoes a 90° rotation from *parallel* to *perpendicular* relative to the Azo-PI alignment direction with increasing Azo-PI alignment. The much smaller DR of pentacene than that of Azo-PI is mainly due to its zigzag molecular packing [see Fig. 5(d)].

XRD patterns in Fig. 2(a) show a “thin film phase” of the pentacene films [15]. With increasing LPL exposure, the peak intensity gradually saturates after a sharp increase [e.g., the (001) intensity in Fig. 2(b)], while their FWHM keeps almost constant with a variation of less than 10%. The films consist of layered grains with a monolayer (ML) height of ~1.6 nm (Fig. 3). Interestingly, some linear chainlike islands are also present. Since no terraces can be discerned from the height profile of the linear islands, we deduce that they are amorphous or have a low degree of order, and the XRD patterns should mainly result from the layered grains. The quantity of the linear islands increases with LPL exposure and the islands are aligned perpendicular to Azo-PI at exposure >5.5 J/cm², implying that the island alignment is induced by the aligned Azo-PI. For the layered grains, a dendritic shape becomes clearer with increasing exposure, and the grain size, which is the circular-area-equivalent-diameter averaged over five AFM images, shows a saturation after a sharp increase.

Motivated by the intriguing correlation between the LPL exposure dependence of Azo-PI DR [Fig. 1(c)], pentacene XRD intensity (Fig. 2) and grain size (Fig. 3), we replot these data in Fig. 4 to get a clearer image of their relationship. To facilitate comparison, here the XRD intensity and grain size of all samples are normalized by assuming the values of the 320 J/cm² sample as 1. The in-plane molecular order parameter $Q_{\Phi} = (A_{\perp} - A_{//})/(A_{\perp} + A_{//})$ instead of the DR is used as a more quantifiable measure of alignment, since for a perfect alignment $|Q_{\Phi}| = 1$ while the DR becomes infinity. Surprisingly, the XRD intensity and the grain size show very similar dependence on $Q_{\Phi}^{\text{Azo-PI}}$ with an exactly the same turning point at $Q_{\Phi}^{\text{Azo-PI}} = 0.4$ (corresponds to 11 J/cm²), which is also the same point at which Q_{Φ}^{pen} begins to increase sharply. This coincidence suggests that the sudden increase of crystallinity and grain size originates from the 90° orientational change of pentacene. Based on these results one can deduce the coexistence of two types of orientations, with

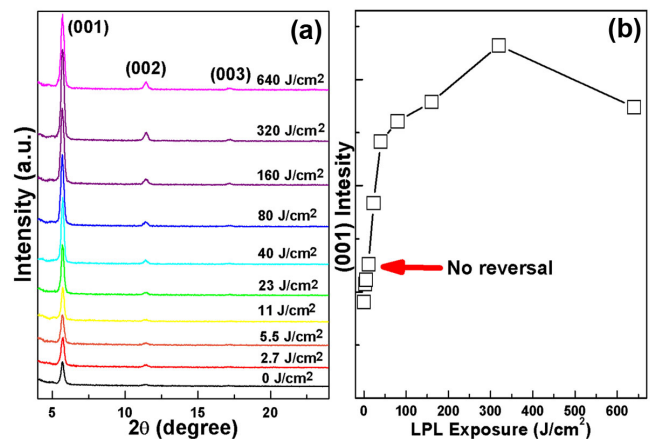


FIG. 2 (color online). (a) XRD patterns of the pentacene films deposited on Azo-PI films with different LPL exposure. (b) LPL exposure dependence of the (001) peak intensity.

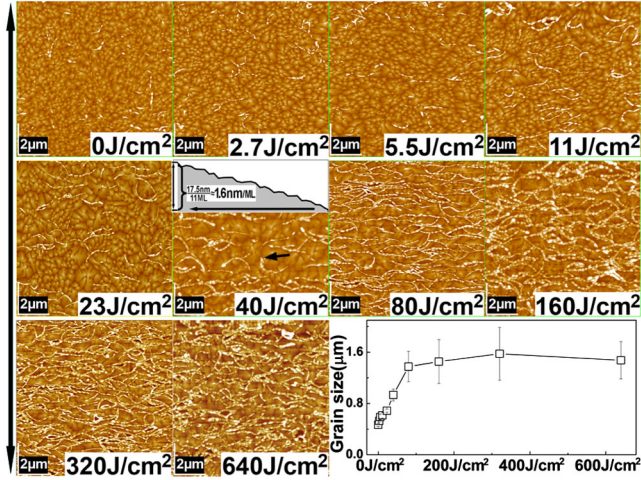


FIG. 3 (color online). AFM images of the pentacene films deposited on Azo-PI films with different LPL exposure. The double arrow in the left side indicates the Azo-PI alignment direction. The inset of the 40 J/cm² sample shows the height profile of the line indicated by the black single arrow, which shows a terrace height of ~ 1.6 nm. LPL exposure dependence of the size of the layered grains is shown at the right bottom.

the aromatic plane on average parallel (*A*-type) or perpendicular (*B*-type) to the Azo-PI alignment direction. We can thus interpret Fig. 4 by a variation of the relative amount of the two types of domains, as schematically illustrated by the white and black area at the bottom of the figure. For the film on untreated Azo-PI, the interaction between pentacene and Azo-PI may induce an *A*-type orientation. However, since the Azo-PI chains are randomly oriented, the pentacene film has no macroscopic in-plane anisotropy, i.e. $Q_{\Phi}^{\text{pen}} = \text{zero}$. For $Q_{\Phi}^{\text{Azo-PI}} \leq 0.4$, the *A*-type orientation is predominant (the *B*-type one is negligible) and Q_{Φ}^{pen} decreases with $Q_{\Phi}^{\text{Azo-PI}}$ since it is derived from the *Z*-axis band (polarized perpendicular to the Azo-PI). The increase in XRD intensity and grain size can be explained by the increased amount (or crystallinity) of the *A*-type orientated domains induced by the increased Azo-PI alignment. For $Q_{\Phi}^{\text{Azo-PI}} > 0.4$, the *A*-type domains decrease while those *B*-type domains increase, leading to the increased Q_{Φ}^{pen} . At $Q_{\Phi}^{\text{Azo-PI}} \approx 0.55$ (~ 33 J/cm²) the two types of domains become equivalent. As a result, Q_{Φ}^{pen} becomes zero, but the XRD intensity and grain size are significantly increased compared to the data of the film on untreated Azo-PI. Above $Q_{\Phi}^{\text{Azo-PI}} = 0.7$ the orientation is almost exclusively the *B*-type. We conclude that the sudden change after $Q_{\Phi}^{\text{Azo-PI}} = 0.4$ is due to a change in the orientation mechanism, which will be discussed in the below.

The GIXD patterns of two typical pentacene samples are shown in Fig. 5(b), where the scattering vector Δk (the diffraction plane normal, see Fig. 5(a)) is parallel to the Azo-PI alignment direction. The corresponding Φ scan profiles taken from the (200) plane at $2\theta\chi = 23.52^\circ$ are shown in Fig. 5(c). Since the Azo-PI backbone is aligned

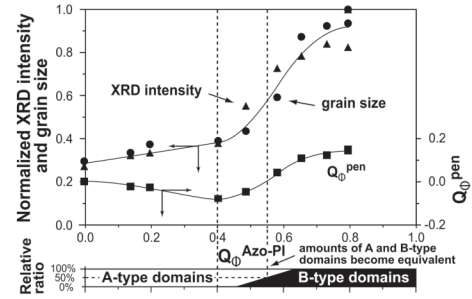


FIG. 4. $Q_{\Phi}^{\text{Azo-PI}}$ dependence of normalized XRD intensity (triangles), normalized grain size (circles) and Q_{Φ}^{pen} (squares). The two epitaxy regimes and the relative ratio of the two types of domains are schematically illustrated by the white and black area at the bottom.

parallel to Δk at $\Phi = \theta\chi = 11.76^\circ$, the two broad peaks centered at $\Phi \approx 102^\circ$ and $\Phi \approx 282^\circ$ (namely a 90° rotation) of the 11 J/cm² sample indicates that the (200) plane [see Fig. 5(d)] is oriented parallel to the Azo-PI alignment direction, agreeing well with the polarized IR data. More interestingly, each broad peak symmetrically splits into two maximums at $\Phi \approx 102 \pm 25^\circ$ and $\Phi \approx 282 \pm 25^\circ$, revealing that the *A*-type orientation predominant in the 11 J/cm² sample actually consists of two types of twinlike oriented domains with the (200) plane deviating by $\pm 25^\circ$ from the Azo-PI alignment direction. The 50° orientation difference matches well with the calculated edge-to-face angle of $\sim 48.1^\circ$ of adjacent pentacene molecules in the thin film phase [16,17]. Therefore, an *A*-type structure can be derived as shown in Fig. 5(d). In each type of the twinlike domains, the molecular plane of either of the two pentacene molecules in a unit cell orients along the Azo-PI alignment direction. The Φ scan profile of the 320 J/cm² sample has a similar shape to that of the 11 J/cm² sample while the peak positions shift $\sim 90^\circ$. This confirms the 90° orientational change. It also reveals twinlike domains of the *B*-type orientation as shown in Fig. 5(e). The higher intensity in the Φ scan of the 320 J/cm² sample than that of the 11 J/cm² sample also confirms an improved in-plane molecular packing order, agreeing well with the higher XRD intensity and larger grain size of the former sample.

The equilibrium molecular orientations are enforced by the relative strengths of several competing factors: (i) topological effects (graphoepitaxy), (ii) van der Waals interactions between pentacene and Azo-PI, and (iii) the availability of geometrical configurations that permit registry between the two layers, i.e., lattice matching. Since the dendritic grains show no anisotropic morphological features, which is common in graphoepitaxy [18], a topological effect should not be predominant. For a low Azo-PI alignment degree, the local lattice spacing of Azo-PI may fluctuate widely. Consequently, lattice matching would have only a minor effect, and the orientation may be mainly achieved by the anisotropic van der Waals inter-

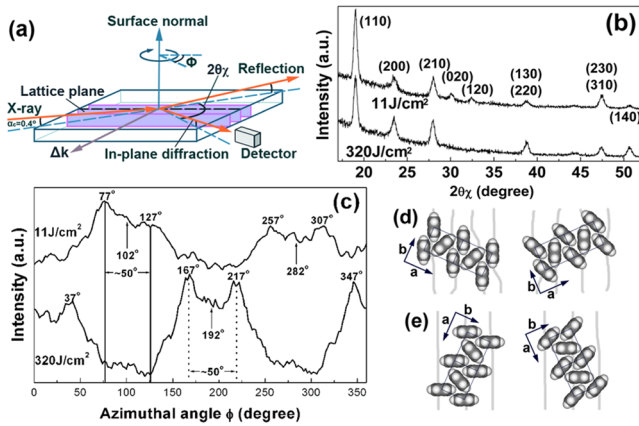


FIG. 5 (color online). (a) Schematic of the x-ray optics for the GIXD measurement. (b) GIXD profiles of the pentacene films on 11 J/cm² and 320 J/cm² exposed Azo-PI films. (c) In-plane azimuthal Φ scan profiles. (d) and (e) schematically illustrate (two unit cells in a - b plane) the A-type and B-type twinlike domains, respectively. Azo-PI molecular chains are indicated by the gray lines.

actions between Azo-PI and individual pentacene molecules, as similar to many OIHE systems with an interface of van der Waals nature and large lattice mismatch [5]. When the Azo-PI is highly aligned, the anisotropic van der Waals interactions are less effective in orienting an entire layer due to lateral interactions between the pentacene molecules, and the role of the substrate orientation should be more important, though still not as effective as in conventional inorganic epitaxy. The undisturbed thin film phase indicates that the intralayer interaction in pentacene film is much stronger than the interlayer interaction between pentacene and the substrate, and the energetic benefit of moving the molecules to ideal commensurate sites cannot overcome the penalty associated with perturbation of the “native” minimum energy of the pentacene. Thus, in the absence of an ideal epitaxial match, the net free energy is minimized for two particular azimuthal orientations, forming a linearly commensurate structure [19] or coincident epitaxy [6] with twinlike domains. Under such a relaxed epitaxial condition, only a subgroup of lattice points of the overlayer and substrate are in perfect registry [5,6,9].

According to Fig. 4, $Q_{\Phi}^{\text{Azo-PI}} = 0.4$ is a threshold value for the predominant orientation mechanism changes from being controlled by anisotropic van der Waals interactions to being controlled by coincident epitaxy. The much sharper increase in XRD intensity and grain size above $Q_{\Phi}^{\text{Azo-PI}} = 0.4$ indicates that the alignment of crystallographic axis in the latter case has a more significant effect in improving the pentacene molecular packing order. For both cases, we may presume that at first the orientation is achieved in the first ML of pentacene. Then the upper layers are epitaxially grown on the first ML template, leading to a drastic change in the overall molecular orientation.

In summary, we demonstrate a distinct polymer alignment-induced epitaxial transition, the controlling fac-

tor of which is attributed to a change from anisotropic van der Waals interactions to coincident epitaxy. The results imply that the molecular orientation in OOHE can be easily controlled by adjusting the relative strength of competing weak interactions. Considering the weak bondings in organics, this conclusion is expected to be generic and hold in other organic semiconductors too. The finding may provide some new insights in understanding organic semiconductor growth. It also shows a promising approach for tuning the characteristic of the relevant organic devices, thus, opening interesting opportunities for future developments of new organic devices.

This work was supported by JSPS (No. 18360012). A portion of the work was conducted at AIST (“Nanotechnology Network Japan” of MEXT, Japan). The authors thank Dr. J. H. G. Owen for valuable discussion.

*Corresponding author.

dong.guo@epfl.ch

- [1] H. E. Katz, *Chem. Mater.* **16**, 4748 (2004).
- [2] G. Horowitz and M. E. Hajlaoui, *J. Mater. Res.* **19**, 1946 (2004).
- [3] G. Malliaras and R. Friend, *Phys. Today* **58**, No. 5, 53 (2005).
- [4] R. Ruiz, D. Choudhary, B. Nickel, T. Toccoli, K. C. Chang, A. C. Mayer, P. Clancy, J. M. Blakely, R. L. Headrick, S. Iannotta, and G. G. Malliaras, *Chem. Mater.* **16**, 4497 (2004).
- [5] A. Koma, *Prog. Cryst. Growth Charact. Mater.* **30**, 129 (1995).
- [6] D. E. Hooks, T. Fritz, and M. D. Ward, *Adv. Mater.* **13**, 227 (2001).
- [7] S. C. B. Mannsfeld, K. Leo, and T. Fritz, *Phys. Rev. Lett.* **94**, 056104 (2005).
- [8] E. Barrena, D. G. de Oteyza, S. Sellner, H. Dosch, J. O. Osso, and B. Struth, *Phys. Rev. Lett.* **97**, 076102 (2006).
- [9] F. Cicoira, J. A. Miwa, D. F. Perepichka, and F. Rosei, *J. Phys. Chem. A* **111**, 12 674 (2007).
- [10] K. Sakamoto, K. Usami, M. Kikigawa, and S. Ushioda, *J. Appl. Phys.* **93**, 1039 (2003).
- [11] H. Ishida, S. T. Wellinghoff, E. Baer, and J. L. Koenig, *Macromolecules* **13**, 826 (1980).
- [12] D. M. Hudgins and S. A. Sandford, *J. Phys. Chem. A* **102**, 344 (1998).
- [13] Y. Hosoi, K. Okamura, Y. Kimura, H. Ishii, and M. Niwano, *Appl. Surf. Sci.* **244**, 607 (2005).
- [14] D. Ross and R. Aroca, *J. Chem. Phys.* **117**, 8095 (2002).
- [15] I. P. M. Bouchoms, W. A. Schoonveld, J. Vrijmoeth, and T. M. Klapwijk, *Synth. Met.* **104**, 175 (1999).
- [16] S. E. Fritz, S. M. Martin, C. D. Frisbie, M. D. Ward, and M. F. Toney, *J. Am. Chem. Soc.* **126**, 4084 (2004).
- [17] R. Ruiz, A. C. Mayer, G. G. Malliaras, B. Nickel, G. Scoles, A. Kazimirov, H. Kim, R. L. Headrick, and Z. Islam, *Appl. Phys. Lett.* **85**, 4926 (2004).
- [18] H. I. Smith, M. W. Gels, C. V. Thompson, and H. A. Atwater, *J. Cryst. Growth* **63**, 527 (1983).
- [19] F. Grey and J. Bohr, *Appl. Surf. Sci.* **65**, 35 (1993).